Coggon, R.M., Teagle, D.A.H., Sylvan, J.B., Reece, J., Estes, E.R., Williams, T.J., Christeson, G.L., and the Expedition 390/393 Scientists
Proceedings of the International Ocean Discovery Program Volume 390/393
publications.iodp.org

Data report: X-ray fluorescence scanning of sediment cores, IODP Expedition 390/393 Site U1560, South Atlantic Transect[1]

Chiara Amadori,[2] Chiara Borrelli,[2] Gail Christeson,[2] Emily Estes,[2] Laura Guertin,[2] Jennifer Hertzberg,[3] Michael R. Kaplan,[2] Ravi Kiran Koorapati,[4] Adriane R. Lam,[2] Christopher M. Lowery,[2] Andrew McIntyre,[2] Julia Reece,[2] Claudio Robustelli Test,[2] Claire M. Routledge,[2] Patricia Standring,[5] Jason B. Sylvan,[2] Mary Thompson,[3] Alexandra Villa,[2] Yi Wang,[2] Shu Ying Wee,[2] Trevor Williams,[2] Jesse Yeon,[3] Damon A.H. Teagle,[2] Rosalind M. Coggon,[2] and the Expedition 390/393 Scientists[2]

[1] Amadori, C., Borrelli, C., Christeson, G., Estes, E., Guertin, L., Hertzberg, J., Kaplan, M.R., Koorapati, R.K., Lam, A.R., Lowery, C.M., McIntyre, A., Reece, J., Robustelli Test, C., Routledge, C.M., Standring, P., Sylvan, J.B., Thompson, M., Villa, A., Wang, Y., Wee, S.Y., Williams, T., Yeon, J., Teagle, D.A.H., Coggon, R.M., and the Expedition 390/393 Scientists, 2024. Data report: X-ray fluorescence scanning of sediment cores, IODP Expedition 390/393 Site U1560, South Atlantic Transect. In Coggon, R.M., Teagle, D.A.H., Sylvan, J.B., Reece, J., Estes, E.R., Williams, T.J., Christeson, G.L., and the Expedition 390/393 Scientists, South Atlantic Transect. Proceedings of the International Ocean Discovery Program, 390/393: College Station, TX (International Ocean Discovery Program). https://doi.org/10.14379/iodp.proc.390393.205.2024
[2] **Expedition 390/393 Scientists' affiliations.** Correspondence author: **chiara.amadori@unipv.it**
[3] Texas A&M University, United States.
[4] Binghamton University, United States.
[5] University of Texas at Austin, United States.

Keywords
International Ocean Discovery Program, IODP, *JOIDES Resolution*, Expedition 390, Expedition 393, Expedition 395E, South Atlantic Transect, Site U1560, X-ray fluorescence core scanning, XRF core scanning, Middle Miocene Climatic Optimum, Miocene, Pliocene, Pleistocene, Neogene

Supplementary material

References (RIS)

MS 390393-205
Received 14 October 2023
Accepted 30 January 2024
Published 19 April 2024

Abstract

International Ocean Discovery Program (IODP) Expeditions 390C, 395E, 390, and 393 recovered deepwater sediments from the western flank of the Mid-Atlantic Ridge in the South Atlantic Ocean along the South Atlantic Transect (SAT) at ~31°S. Collectively, these expeditions recovered ~2 km of sediment cores that have the potential to capture key features of Cenozoic climate change. In this report, we show semiquantitative bulk elemental results from X-ray fluorescence (XRF) scanning of the sediment cores from IODP Site U1560 recovered during Expeditions 395E and 393. The oceanic basement at this site is ~15 My old, making it the second youngest of the SAT sites located west of the Mid-Atlantic Ridge. Here, XRF data are compared with pass-through magnetic susceptibility and natural gamma radiation of the sediment cores, measured aboard *JOIDES Resolution*. The resulting trends and correlations highlight elemental variations through time, mainly reflecting lithologic and compositional differences.

At Site U1560, Ca counts reflect the occurrence of nannofossil ooze, which is the dominant lithology for the whole site. In the Miocene-aged Lithologic Units IE–IA from 140 to 50 m core composite depth below seafloor (CCSF), several high-intensity spikes of detrital elements (i.e., Fe, Ti, Al, Si, and Zr) correspond to intervals of clay-rich nannofossil ooze. Detrital elemental counts in the entire Pliocene record (50 to ~25 m CCSF) are the lowest. A sharp shift is observed at the Pliocene/Pleistocene boundary at ~25 m CCSF, with the uppermost Pleistocene record showing high-frequency and high-intensity variations in siliciclastic elements, which correlates well with the pass-through magnetic susceptibility.

1. Introduction

The South Atlantic Ocean has been of special interest from the beginning of the Deep Sea Drilling Project (e.g., Leg 3 in the late 1960s), given its primary role in confirming the hypothesis of seafloor spreading and plate tectonics (Scientific Party, 1970). A transect near the Leg 3 sites comprising new drill sites across the western flank of the Mid-Atlantic Ridge, the South Atlantic Transect

(SAT) (**Coggon et al.**, 2024), was completed in 2020–2022 during International Ocean Discovery Program (IODP) Expeditions 390C, 395E, 390, and 393. In a modern concept, the acquired well-log data and recovery of both oceanic basement and deepwater sediments will significantly contribute to answering fundamental questions regarding Cenozoic climate change (such as the Eocene–Oligocene Transition and hyperthermal events), paleoceanography (i.e., bottom currents and water mass chemical balance), and fluid-rock interaction (hydrothermal activity) over the last ~61 My.

Site U1560, located ~315 km west of the Mid-Atlantic Ridge (30°24.2057′S, 16°55.3702′W; 3723 meters below sea level [mbsl]), comprises adjacent Holes U1560A, U1560B, and U1560C cored during Expeditions 395E and 393 (Williams et al., 2021; Teagle et al., 2023) (Figure **F1**). Site U1560 is the second youngest site of the SAT after Site U1559 (**Coggon et al.**, 2024; **Robustelli Test et al.**, 2024) and comprises sediments deposited over the last ~15 My, including the Middle Miocene Climatic Optimum and the Pliocene–Pleistocene Transition.

Holes U1560A and U1560C recovered 120 m and 129 m, respectively, of the same Miocene–Holocene stratigraphy, which is about twice as thick as the sediment record at SAT Site U1559 located 185 km east on ~6.6 Ma ocean crust.

At Site U1560, the Miocene–Holocene sediments are divided into five lithologic units (IA–IE) (Teagle et al., 2023). This division is based on lithologic differences mostly related to the color and/or clay content, although the dominant lithology is nannofossil ooze. Some layers in Unit IE are also organic rich. Unit IA comprises ~49 m of Pleistocene to Late Miocene (Messinian) predominantly light pink nannofossil ooze with variable foraminifera and clay. Unit IB comprises ~11 m of Late Tortonian–Messinian light brown nannofossil ooze with clay. Unit IC comprises ~25 m of Tortonian pink to light brown nannofossil ooze with clay. Unit ID comprises ~12 m of Serravallian–Tortonian brown clayey nannofossil ooze. Finally, Unit IE comprises ~22 m of brown organic-rich nannofossil ooze with clay dated from Langhian to Serravallian in age. All ages are based on biostratigraphic (calcareous nannofossil and planktonic foraminifera) and magnetostratigraphic data (Teagle et al., 2023).

X-ray fluorescence (XRF) core scanning across all SAT sites, including Site U1560, aimed to produce a dedicated semiquantitative data set of elements (Penkrot et al., 2018; Taylor et al., 2022) often used for paleoceanographic interpretation (e.g., Croudace and Rothwell, 2015). The bulk elemental characterization of the lithologic units will improve their lithologic description and help with correlation across the SAT. This was possible because the chosen sampling resolution allowed for the production of a high-resolution record of the entire sedimentary section.

This data report contains all quality-controlled XRF data produced during programmatic scanning of Site U1560 sediments. Basic counts of major elements are plotted against stratigraphy and

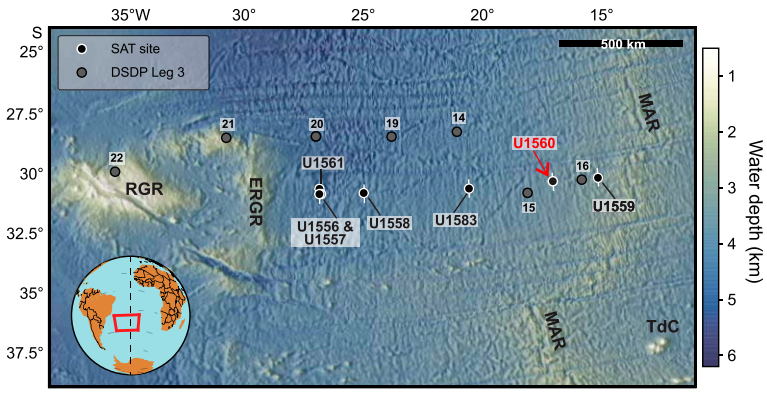

Figure F1. Expedition 390/393 drill site locations. Deep Sea Drilling Program Leg 3 sites are included for reference. Figure modified from Teagle et al. (2023). RGR = Rio Grande Rise, ERGR = Eastern Rio Grande Rise, MAR = Mid-Atlantic Ridge, TdC = Tristan de Cunha hotspot.

combined with pass-through magnetic susceptibility (MS) and natural gamma radiation (NGR) measured on whole-round cores aboard *JOIDES Resolution* during the expeditions.

2. Methods and materials

Archive section halves comprising the splice for Site U1560 were scanned at the IODP Gulf Coast Repository (GCR) in College Station, Texas (USA). The analysis was performed using the third-generation Avaatech XRF core scanner (XRF 1). This instrument is fitted with a water-cooled, 100 W rhodium side-window X-ray tube, a Brightspec SiriusSD silicon drift detector, and a Topaz-X high-resolution digital multichannel analyzer. Each archive section half was scanned at three excitation levels to measure different elements: 10 kV (6 s count time; no filter) for major and minor elements (including Al, Si, K, Ca, Ti, Mn, Fe, Cr, P, S, and Mg), 30 kV (6 s count time; with a thick Pd filter) for heavier major and minor elements and geologically relevant trace elements (i.e., Ca, Ti, Mn, Fe, Ni, Sr, Rb, Zr, and Zn), and 50 kV (10 s count time; with a Cu filter) for heavier trace elements (i.e., Sr, Rb, Zr, and Ba). The cross-core and downcore slits were set to 12 and 10 mm, respectively. Current was set to 0.15, 1.24, and 0.75 mA for the 10, 30, and 50 kV scans, respectively.

Detection limits for some elements for clay-rich sediment measured at 10 kV with no filter and a 20 s count time are Al 0.2%, Si 0.1%, P 0.05%, S 0.05%, K 0.04%, Ca 0.02%, Ti 0.05%, Mn 100 ppm, Fe 45 ppm, Sr 5 ppm, Zr 20 ppm, and Ba 40 ppm.

2.1. Core preparation

The archive section halves are stored in the refrigerated core repository at 4°C but were thermally equilibrated to room temperature before being prepared for XRF scanning. Warming before adding the film helps prevent condensation on the film and is done because condensation absorbs X-ray spectra, which results in biases, particularly for light elements (Kido et al., 2006).

The end caps were partially cut and reshaped to allow the detector to fit and measure the first and the last point on the section (i.e., the closest ones to the edges). The split face of each section was gently scraped clean with a glass slide to expose fresh sediments, remove mold, and create smooth flat surfaces for the detector to adhere better. The scraping was performed perpendicular to the core splitting line (parallel to sedimentary bedding) to ensure that no material was moved from its stratigraphic position. The glass slides were cleaned with water and lint-free wipes between each scrape. Several lint-free wipes were laid across any soupy intervals to soak up excess water. Once the section halves had been prepared, a 4 µm thick Ultralene film was laid on the exposed surface and taped to the edges of the core liner to prevent contamination of the XRF detector as it moved from the top to the bottom of the section. Care was taken to prevent air pockets from forming along the central zone of the core sections, which is the area scanned by the XRF detector.

2.2. Sample selection

All sections of the Site U1560 shipboard splice from Holes U1560A and U1560C were scanned at a 2 cm resolution for a total spliced depth of 140 m CCSF. The uppermost data recorded is 2 cm below the top of the section, and the lowest point is set as close as possible to the bottom. For a preliminary overview of the exact points scanned with the XRF detector, a 3D-printed replica of the scanning window was used to examine each core at 2 cm intervals. This step was fundamental to carefully select good XRF sample spots and avoid section voids (due to sampling that occurred shipboard, for instance), cracks from water loss, rough surfaces, or intervals affected by intense drilling disturbance (biscuiting) and the presence of drilling mud. Drilling disturbance is often present in sediments cored using the extended core barrel (XCB) system. When a sample spot was unsuitable for any of the above mentioned reasons, it was manually moved a few centimeters either up- or downsection to maintain the targeted resolution, if possible, or simply skipped if there was no suitable spot nearby.

2.3. Quality control

The quality control associated with XRF data acquisition consists of running standards at all three excitation levels (10, 30, and 50 kV) before and at the end of each scanning day to monitor instrument performance and check for possible contamination on the film. The initial run is performed to warm up the machine and includes 20 replicates per excitation level. Replicates are not performed at the end of the scanning day, and the single-run setup is used instead.

Raw spectral peaks were processed into peak areas and exported as counts per second for different elements using the Brightspec XRF spectral processing software program bAxil. To provide data quality control and remove bad measurements resulting from gaps between the sensor and the core, we excluded sample points with throughput values of less than 150,000 counts/s at the 10 kV scan and sample points with positive Ar value, which indicated the detector was actually measuring ambient air. This quality control was carried out using a code that was written for the program R (R Core Team, 2023) and is available online (**https://github.com/Ravikiran2316/IODP-Exp.-390-393-XRF**).

Typically, individual elemental values within two standard deviations of zero are also deleted from XRF data sets, but because that will vary from element to element in a single sample (e.g., Ti counts may be significant, whereas Ni counts may not be) we did not remove any data points based on this criterion but rather left this up to the end user of the data. Complementary data sets have been developed for all the other sites, as follows: U1556 (**Wang et al.**, 2024), U1557 (**Lowery et al.**, 2024), U1558 (**Villa et al.**, 2024), U1561 (**Routledge et al.**, 2024), U1559 (**Robustelli Test et al.**, 2024), and U1583 (**Lam et al.**, 2024).

3. Results

3.1. Correlation between elements

To test the strength of correlation among common elements associated with pelagic (carbonate mud–rich) and terrigenous-sourced sediments (e.g., Croudace and Rothwell, 2015) at Site U1560, we plotted those elements against each other (Figure **F2**). Expected positive correlations exist for terrigenous-derived major elements like Fe and Ti, Fe and K, and Ti and Si. Anticorrelations were observed for pelagic and terrigenous-sourced elements like Ca and Fe, Ca and Ti, and Ca and Si.

To determine the statistical dependence between the rankings of two variables and thus which elements correlate with each other, we conducted a Spearman's rank correlation (Figure **F3**). The strongest correlations ($\rho > 0.85$) are among the terrigenous-sourced elements like Mn, Al, Fe, Zr, Si, Ti, and K. The weakest correlations are between Ca, Sr, Ni, Ba, S, and Br against the majority of other elements. Elements that are generally indicative of productivity such as Si, Ba, and Sr mostly have negative ($\rho < -0.35$) or very weak positive ($\rho = 0.01$) correlations with Ca. Sr has a positive but low ($\rho < 0.3$) correlation with all elements except Ba, with which it shows a very weak ($\rho = -0.01$) correlation.

The weakest positive correlations ($\rho < 0.15$) include those between Sr and Ni, Sr and Br, Ba and Br, Mn and Br, Zr and S, Ti and S, K and Ni, and Si and Ni. The most anticorrelated element couples ($\rho < -0.15$) include Ti and Ca ($\rho = -0.51$) and K and Ca ($\rho = -0.42$). Additionally, Fe and Ca, Ca and Sr, and Zr and Ca are negatively correlated ($\rho > -0.4$).

3.2. Stratigraphic trends

Ca shows homogeneously high counts downhole, which is typical of carbonate-rich sediments and nannofossil ooze, although multiple shifts toward lower values are coincident with positive prominent peaks in MS, NGR, and detrital elements (Figure **F4**).

Between 130 and 140 m CCSF (Lithologic Unit IE), there are high-frequency and high-amplitude variations in MS, Fe counts, and other detrital elements. This interval is dated to the Middle Miocene, between 14 and 15 Ma. The rest of the Miocene lithologic units (ID, IC, IB, and the bottom

of IA) contain several isolated but strong peaks in MS, NGR, Fe, Ti, Al, Si, K, and Zr, and these always correspond to intervals of clayey nannofossil ooze.

In the Pliocene portion of Unit IA, mean overall downhole trends and detrital component counts display an abrupt change toward minimum values (Figure **F4**). Ca counts present three large excursions with two relative minima at ~30 and ~40 m CCSF. No other element correlates with this Ca pattern.

The uppermost Pleistocene Unit IA is instead characterized by the sharp return of high-frequency, relatively high amplitude oscillations of MS, NGR, and terrigenous-sourced element counts. These element peaks seem to increase in amplitude upsection, whereas the large oscillations in Ca counts seem to record decreasing minimum values upsection.

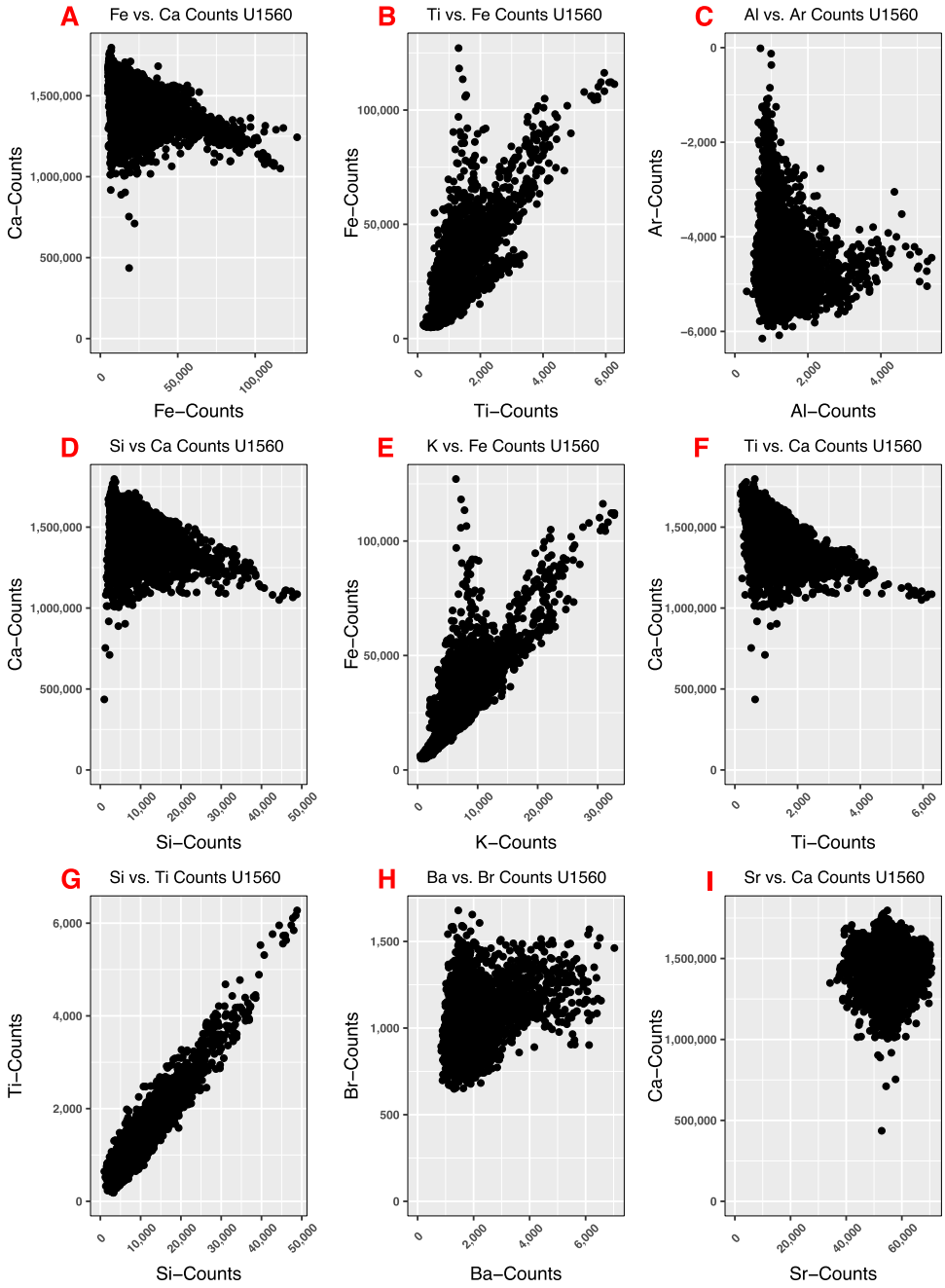

Figure F2. Crossplots of XRF raw counts of selected elements, Site U1560. See Figure F3 for Spearman's rank correlation.

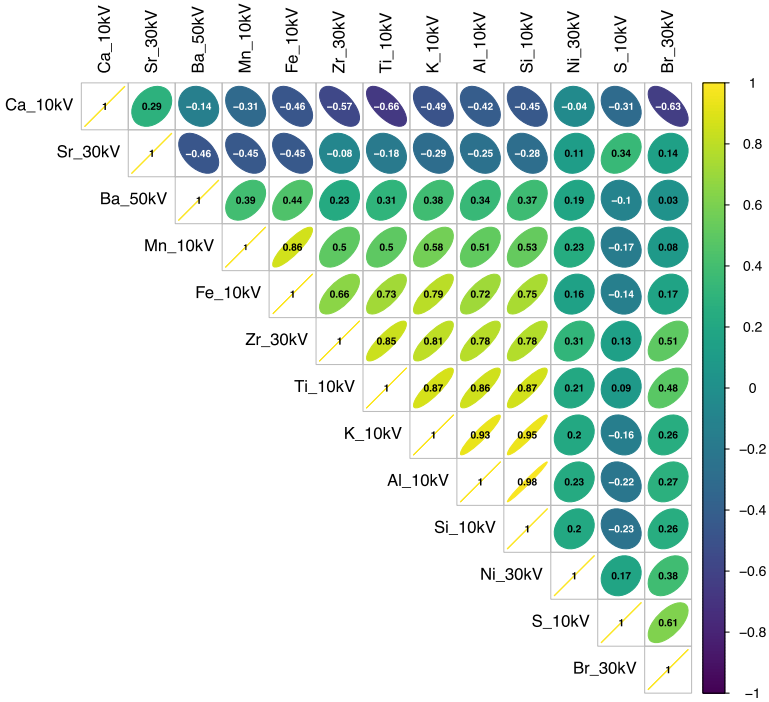

Figure F3. Correlogram of elements above detection limits (>1000 counts/s), Site U1560. Black and white numbers = Spearman's rank correlation coefficients. Correlation is shown on a color gradient from dark blue (ρ = −1, negative correlation) to yellow (ρ = 1, positive correlation). Greater ellipticity of the ellipse in each correlogram grid represents a stronger correlation.

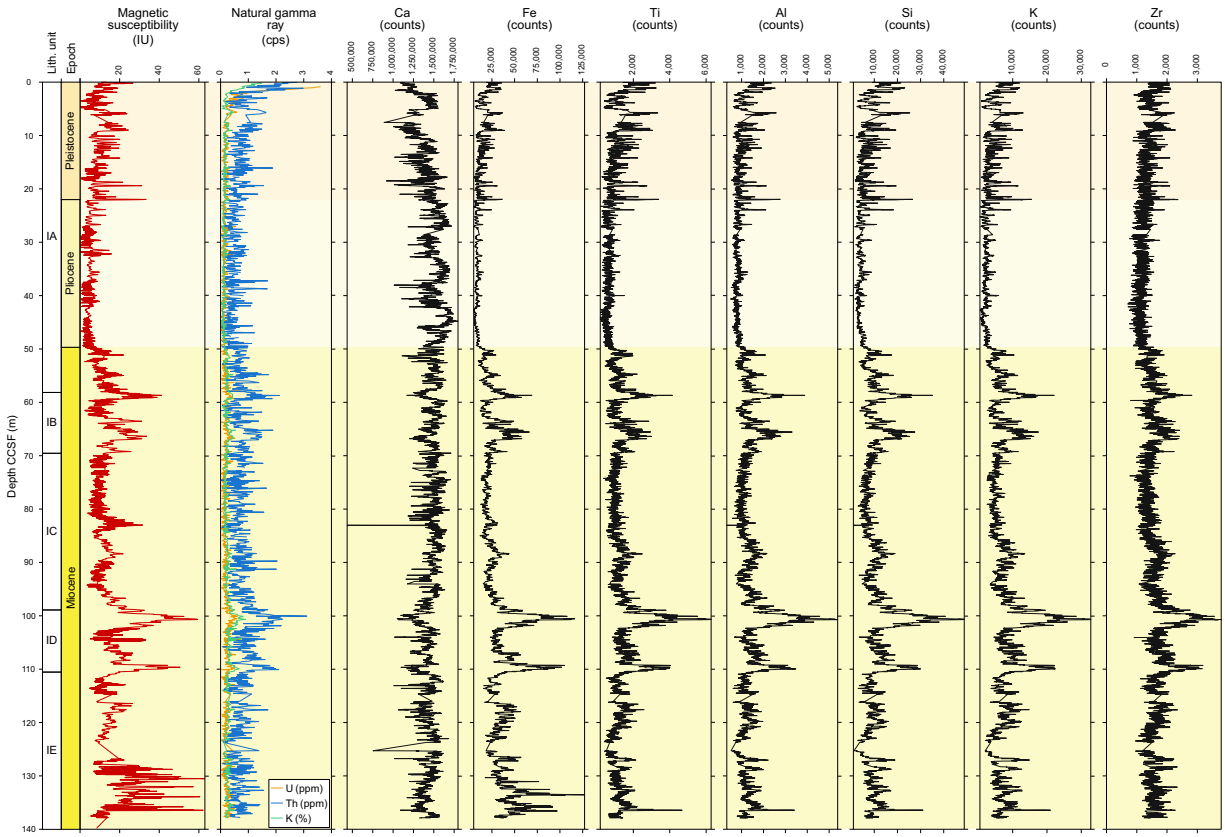

Figure F4. Magnetic susceptibility, spectral NGR, and scanning XRF counts of selected elements, Site U1560. NGR core data are scaled to the concentrations of the individual elements: U (parts per million), Th (parts per million), and K (percent). IU = instrument units, cps = counts per second.

3.3. Data availability

XRF data at all three excitation levels (10, 30, and 50 KV) are included here in XRF in **Supplementary material** and permanently archived at PANGAEA (**https://Pangea.de**).

Complementary data sets have been developed for all the other sites, as follows: U1556 (**Wang et al.**, 2024), U1557 (**Lowery et al.**, 2024), U1558 (**Villa et al.**, 2024), U1561 (**Routledge et al.**, 2024), U1559 (**Robustelli Test et al.**, 2024), and U1583 (**Lam et al.**, 2024).

The R Code used for quality control to remove spurious throughput and Ar values can be found on GitHub (**https://github.com/Ravikiran2316/IODP-Exp.-390-393-XRF**).

4. Acknowledgments

We are grateful to the crew, staff, and technicians of *JOIDES Resolution* for Expeditions 390C, 395E, 390, and 393, as well as the technicians and staff at the GCR, particularly Michelle Penkrot. XRF scans reported here comprise the programmatic scanning for Expeditions 390C, 395E, 390, and 393 and were funded by the National Science Foundation (NSF) in agreement with the US Science Support Program (USSSP). We also acknowledge XRF scanning travel support for US scientists administered by USSSP and funding to E.R. Estes and T.J. Williams through NSF award OCE1326927. We also acknowledge travel support from ECORD for European scientists. The authors wish to thank Molly Patterson for comments and edits that strengthened this data report.

References

Amadori, C., Borrelli, C., Christeson, G., Estes, E., Guertin, L., Hertzberg, J., Kaplan, M.R., Koorapati, R.K., Lam, A.R., Lowery, C.M., McIntyre, A., Reece, J., Robustelli Test, C., Routledge, C.M., Standring, P., Sylvan, J.B., Thompson, M., Villa, A., Wang, Y., Wee, S.Y., Williams, T., Yeon, J., Teagle, D.A.H., Coggon, R.M., and the Expedition 390/393 Scientists, 2024. Supplementary material, **https://doi.org/10.14379/iodp.proc.390393.205supp.2024**. In Amadori, C., Borrelli, C., Christeson, G., Estes, E., Guertin, L., Hertzberg, J., Kaplan, M.R., Koorapati, R.K., Lam, A.R., Lowery, C.M., McIntyre, A., Reece, J., Robustelli Test, C., Routledge, C.M., Standring, P., Sylvan, J.B., Thompson, M., Villa, A., Wang, Y., Wee, S.Y., Williams, T., Yeon, J., Teagle, D.A.H., Coggon, R.M., and the Expedition 390/393 Scientists, Data report: X-ray fluorescence scanning of sediment cores, IODP Expedition 390/393 Site U1560, South Atlantic Transect. In Coggon, R.M., Teagle, D.A.H., Sylvan, J.B., Reece, J., Estes, E.R., Williams, T.J., Christeson, G.L., and the Expedition 390/393 Scientists, South Atlantic Transect. Proceedings of the International Ocean Discovery Program, 390/393: College Station, TX (International Ocean Discovery Program).

Coggon, R.M., Teagle, D.A.H., Sylvan, J.B., Reece, J., Estes, E.R., Williams, T.J., Christeson, G.L., Aizawa, M., Albers, E., Amadori, C., Belgrano, T.M., Borrelli, C., Bridges, J.D., Carter, E.J., D'Angelo, T., Dinarès-Turell, J., Doi, N., Estep, J.D., Evans, A., Gilhooly, W.P., III, Grant, L.C.J., Guérin, G.M., Harris, M., Hojnacki, V.M., Hong, G., Jin, X., Jonnalagadda, M., Kaplan, M.R., Kempton, P.D., Kuwano, D., Labonte, J.M., Lam, A.R., Latas, M., Lowery, C.M., Lu, W., McIntyre, A., Moal-Darrigade, P., Pekar, S.F., Robustelli Test, C., Routledge, C.M., Ryan, J.G., Santiago Ramos, D., Shchepetkina, A., Slagle, A.L., Takada, M., Tamborrino, L., Villa, A., Wang, Y., Wee, S.Y., Widlansky, S.J., Yang, K., Kurz, W., Prakasam, M., Tian, L., Yu, T., and Zhang, G., 2024. Site U1559. In Coggon, R.M., Teagle, D.A.H., Sylvan, J.B., Reece, J., Estes, E.R., Williams, T.J., Christeson, G.L., and the Expedition 390/393 Scientists, South Atlantic Transect. Proceedings of the International Ocean Discovery Program, 390/393: College Station, TX (International Ocean Discovery Program). **https://doi.org/10.14379/iodp.proc.390393.109.2024**

Croudace, I.W., and Rothwell, R.G. (Eds.), 2015. Micro-XRF Studies of Sediment Cores: Applications of a non-destructive tool for the environmental sciences: (Springer Dordrecht). **https://doi.org/10.1007/978-94-017-9849-5**

Kido, Y., Koshikawa, T., and Tada, R., 2006. Rapid and quantitative major element analysis method for wet fine-grained sediments using an XRF microscanner. Marine Geology, 229(3–4):209–225. **https://doi.org/10.1016/j.margeo.2006.03.002**

Lam, A.R., Amadori, C., Borrelli, C., Christeson, G., Estes, E., Guertin, L., Hertzberg, J., Kaplan, M.R., Koorapati, R.K., Lowery, C.M., McIntyre, A., Reece, J.S., Robustelli Test, C., Routledge, C.M., Standring, P., Sylvan, J.B., Thompson, M., Villa, A., Wang, Y., Wee, S.Y., Williams, T., Yeon, J., Teagle, D.A.H., Coggon, R.M., and the Expedition 390/393 Scientists, 2024. Data report: X-ray fluorescence scanning of sediment cores, IODP Expedition 390/393 Site U1583, South Atlantic Transect. In Coggon, R.M., Teagle, D.A.H., Sylvan, J.B., Reece, J., Estes, E.R., Williams, T.J., Christeson, G.L., and the Expedition 390/393 Scientists, South Atlantic Transect. Proceedings of the International Ocean Discovery Program, 390/393: College Station, TX (International Ocean Discovery Program). **https://doi.org/10.14379/iodp.proc.390393.202.2024**

Lowery, C.M., Amadori, C., Borrelli, C., Christeson, G., Estes, E., Guertin, L., Hertzberg, J., Kaplan, M.R., Koorapati, R.K., Lam, A.R., McIntyre, A., Reece, J., Robustelli Test, C., Routledge, C.M., Standring, P., Sylvan, J.B., Thompson, M., Villa, A., Wang, Y., Wee, S.Y., Williams, T., Yeon, J., Teagle, D.A.H., Coggon, R.M., and the Expedition 390/393 Scientists, 2024. Data report: X-ray fluorescence scanning of sediment cores, IODP Expedition 390/393 Site U1557,

South Atlantic Transect. In Coggon, R.M., Teagle, D.A.H., Sylvan, J.B., Reece, J., Estes, E.R., Williams, T.J., Christeson, G.L., and the Expedition 390/393 Scientists, South Atlantic Transect. Proceedings of the International Ocean Discovery Program, 390/393: College Station, TX (International Ocean Discovery Program). **https://doi.org/10.14379/iodp.proc.390393.201.2024**

Penkrot, M.L., Jaeger, J.M., Cowan, E.A., St-Onge, G., and LeVay, L., 2018. Multivariate modeling of glacimarine lithostratigraphy combining scanning XRF, multisensory core properties, and CT imagery: IODP Site U1419. Geosphere, 14(4):1935–1960. **https://doi.org/10.1130/GES01635.1**

R Core Team, 2023. R: A language and environment for statistical computing. R Foundation for Statistical Computing. **https://www.r-project.org/**

Robustelli Test, C., Amadori, C., Borrelli, C., Christeson, G., Estes, E., Guertin, L., Hertzberg, J., Kaplan, M.R., Koorapati, R.K., Lam, A.R., Lowery, C.M., McIntyre, A., Reece, J., Routledge, C.M., Standring, P., Sylvan, J.B., Thompson, M., Villa, A., Wang, Y., Wee, S.Y., Williams, T., Yeon, J., Teagle, D.A.H., Coggon, R.M., and the Expedition 390/393 Scientists, 2024. Data report: X-ray fluorescence scanning of sediment cores, IODP Expedition 390/393 Site U1559, South Atlantic Transect. In Coggon, R.M., Teagle, D.A.H., Sylvan, J.B., Reece, J., Estes, E.R., Williams, T.J., Christeson, G.L., and the Expedition 390/393 Scientists, South Atlantic Transect. Proceedings of the International Ocean Discovery Program, 390/393: College Station, TX (International Ocean Discovery Program). **https://doi.org/10.14379/iodp.proc.390393.204.2024**

Routledge, C.M., Amadori, C., Borrelli, C., Christeson, G., Estes, E., Guertin, L., Hertzberg, J., Kaplan, M.R., Koorapati, R.K., Lam, A.R., Lowery, C.M., McIntyre, A., Reece, J., Robustelli Test, C., Standring, P., Sylvan, J.B., Thompson, M., Villa, A., Wang, Y., Wee, S.Y., Williams, T., Yeon, J., Teagle, D.A.H., Coggon, R.M., and the Expedition 390/393 Scientists, 2024. Data report: X-ray fluorescence scanning of sediment cores, IODP Expedition 390/393 Site U1561, South Atlantic Transect. In Coggon, R.M., Teagle, D.A.H., Sylvan, J.B., Reece, J., Estes, E.R., Williams, T.J., Christeson, G.L., and the Expedition 390/393 Scientists, South Atlantic Transect. Proceedings of the International Ocean Discovery Program, 390/393: College Station, TX (International Ocean Discovery Program). **https://doi.org/10.14379/iodp.proc.390393.207.2024**

Scientific Party, 1970. Introduction. In Maxwell, A.E., et al., Initial Reports of the Deep Sea Drilling Project. 3: Washington, DC (US Government Printing Office), 7–9. **https://doi.org/10.2973/dsdp.proc.3.101.1970**

Taylor, S.P., Patterson, M.O., Lam, A.R., Jones, H., Woodard, S.C., Habicht, M.H., Thomas, E.K., and Grant, G.R., 2022. Expanded North Pacific subtropical gyre and heterodyne expression during the Mid-Pleistocene. Paleoceanography and Paleoclimatology, 37(5):e2021PA004395. **https://doi.org/10.1029/2021PA004395**

Teagle, D.A.H., Reece, J., Coggon, R.M., Sylvan, J.B., Christeson, G.L., Williams, T.J., Estes, E.R., and the Expedition 393 Scientists, 2023. Expedition 393 Preliminary Report: South Atlantic Transect 2. International Ocean Discovery Program. **https://doi.org/10.14379/iodp.pr.393.2023**

Villa, A., Amadori, C., Borrelli, C., Christeson, G., Estes, E., Guertin, L., Hertzberg, J., Kaplan, M.R., Koorapati, R.K., Lam, A.R., Lowery, C.M., McIntyre, A., Reece, J., Robustelli Test, C., Routledge, C.M., Standring, P., Sylvan, J.B., Thompson, M., Wang, Y., Wee, S.Y., Williams, T., Yeon, J., Teagle, D.A.H., Coggon, R.M., and the Expedition 390/393 Scientists, 2024. Data report: X-ray fluorescence scanning of sediment cores, IODP Expedition 390/393 Site U1558, South Atlantic Transect. In Coggon, R.M., Teagle, D.A.H., Sylvan, J.B., Reece, J., Estes, E.R., Williams, T.J., Christeson, G.L., and the Expedition 390/393 Scientists, South Atlantic Transect. Proceedings of the International Ocean Discovery Program, 390/393: College Station, TX (International Ocean Discovery Program). **https://doi.org/10.14379/iodp.proc.390393.203.2024**

Wang, Y., Amadori, C., Borrelli, C., Christeson, G., Estes, E., Guertin, L., Hertzberg, J., Kaplan, M.R., Koorapati, R.K., Lam, A.R., Lowery, C.M., McIntyre, A., Reece, J., Robustelli Test, C., Routledge, C.M., Standring, P., Sylvan, J.B., Thompson, M., Villa, A., Wee, S.Y., Williams, T., Yeon, J., and the Expedition 390/393 Scientists, 2024. Data report: X-ray fluorescence scanning of sediment cores, IODP Expedition 390/393 Site U1556, South Atlantic Transect. In Coggon, R.M., Teagle, D.A.H., Sylvan, J.B., Reece, J., Estes, E.R., Williams, T.J., Christeson, G.L., and the Expedition 390/393 Scientists, South Atlantic Transect. Proceedings of the International Ocean Discovery Program, 390/393: College Station, TX (International Ocean Discovery Program). **https://doi.org/10.14379/iodp.proc.390393.206.2024**

Williams, T., Estes, E.R., Rhinehart, B., Coggon, R.M., Sylvan, J.B., Christeson, G.L., and Teagle, D.A.H., 2021. Expedition 395E Preliminary Report: Complete South Atlantic Transect Reentry Systems. International Ocean Discovery Program. **https://doi.org/10.14379/iodp.pr.395E.2021**